SPIRE

Straylight model update

Draft 0.2 notes

Author: A.G.Richards, Optical Systems Group, RAL

Date: 21 June, 2000-06-21

1. INTRODUCTION

The SPIRE instrument CODEV and APART models have been described in SPIRE/RAL/N0044, 25/9/98. That document described an earlier photometer design (PHOT126B) matched to an earlier telescope design. The APART model of SPIRE was subsequently incorporated into a full FIRST payload Module/Focal Plane Unit straylight model detailed in SPIRE/RAL/N/0101.01. With the evolution of the telescope design and the designs for the SPIRE photometer and spectrometer, the APART model is in the process of being updated. However, some results from the APART analysis of this earlier model are still useful and are reproduced in section 3 below.

The latest instrument optical designs, identified as PH153 (photometer) and SP501 (spectrometer) have already been translated into CODEV form and are now being used to determine geometrical optical beam envelopes in all optical spaces from the detectors to space. These can now be smoothly integrated with the mechanical structure to ensure clearance. Geometrical beam footprints on the major optical components are also now being generated to allow final determination of mirror/filter/beamsplitter/aperture/ sizes. Some of this latest footprint data is presented in section 4.

2. STRAYLIGHT CONCERNS

Of continuing concern has been the estimation and control of the background which each detector sees as a result of steering the detector's field of view using the mirror CM4.[1] It is now proposed that a field stop and thermal filter be located at the telescope focal surface in roughly the location shown in figure 1. An estimate has been made, using the existing APART model of the telescope and cryostat, of the expected thermal load from the telescope+cryostat in the vicinity of this proposed filter. The cryostat emission has been modelled as coming from 5 dummy surfaces, each given an effective emissivity to be expected of cavities having highly reflecting coatings in which multiple reflections play a great part. These dummy surfaces are shown in figure 2, which is taken from SPIRE/RAL/N/0101.01. The surfaces are labelled with their APART identifying numbers.

[1] The latest system for identifying optical surfaces, proposed by Berend Winter, MSSL, is used here.

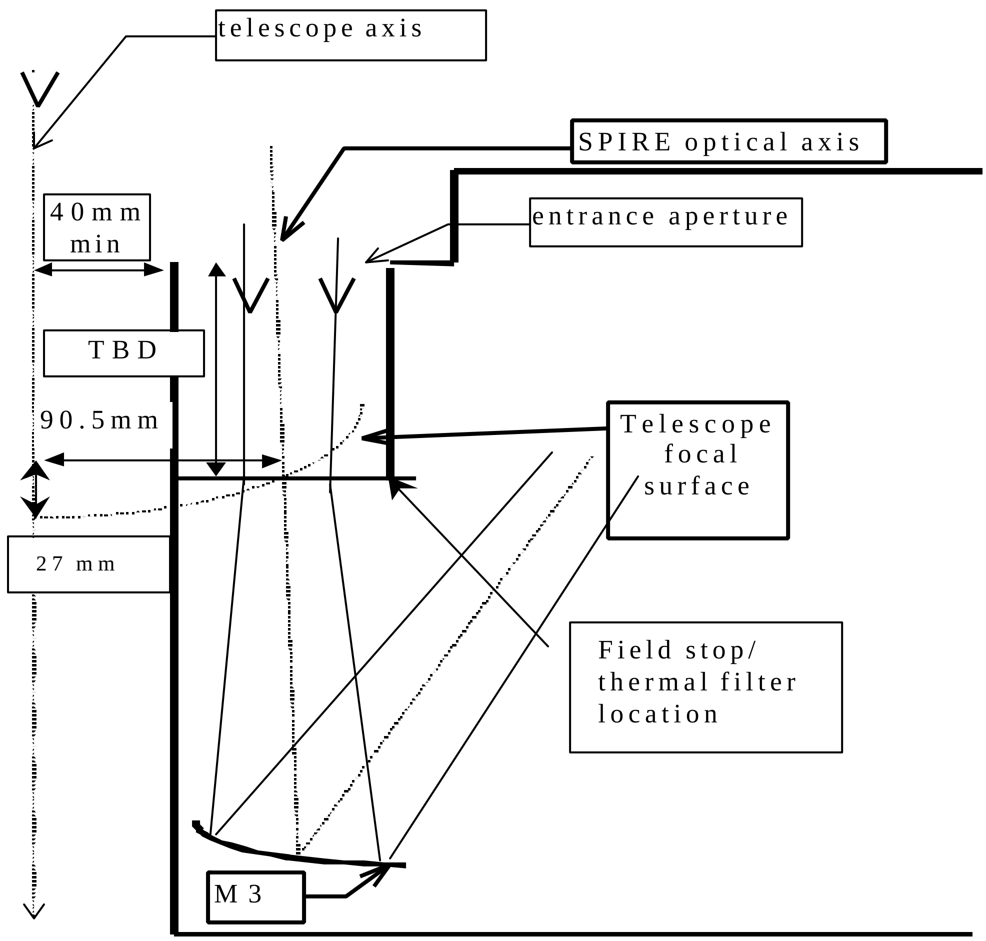

Figure 1 Proposed location for field stop / thermal filter

The rectangular surface located at the telescope focal surface was given dimensions 34 mm by 96 mm. This is very close to the size required to clear the field of view (see later footprint data). The full-bandwidth thermal power reaching it from the telescope side is estimated to be approximately 2.3*10^-5 watt. This divides into about 66% coming from the cryostat (modelled as 5 emitting cylinders centred on the telescope axis, each cylinder having an effective emissivity of 0.29, 0.26, 0.27, 0.25, 0.15 depending on the cylinder length, and having temperatures 14K, 32K, 49K, 64K and 77 K, both sequences being in order of increasing height above the SPIRE instrument), and 33 % from 14 K internal walls surrounding the space between an aperture in the SPIRE cover and the field stop (see figure 1). As modelled, the radiation from the cryostat reaching the focal surface is restricted by a rectangular aperture in a SPIRE cover, but radiation from the inside surfaces of this cover, assumed to be at 14K, also contributes to the load at the rectangular field stop/ thermal filter.

As the APART model of SPIRE is brought up to date, then the thermal loading at other important surfaces in the instruments will be estimated using it.

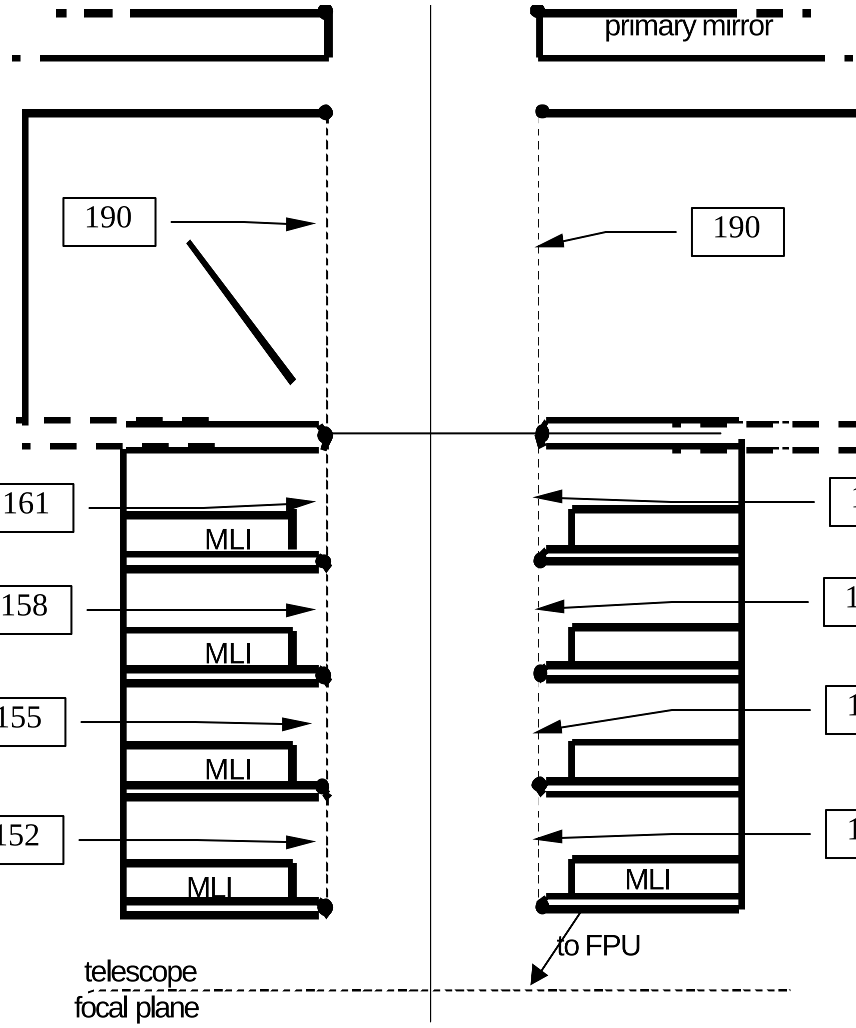

Figure 2 APART model of the cryostat showing dummy radiating surfaces

3. APART ESTIMATES OF SPIRE PHOTOMETER BACKGROUND

The following reasonably accurate estimates or assumptions are made for comparison purposes:

Table 1

Typical total detector area	**2.5^2 sq.cm.**
Throughput to whole detector area (AΩ)	**0.1 cm^2-steradian**
Number of mirrors in optical path at 4K	**6**
Number of mirrors in optical path at 2K	**2**
Mirror emissivity ε	**0.01**

Estimates subsequently made for the total power falling on a detector can be scaled to different detector areas.
It is assumed that we are interested in the total contribution from various sources that reach each detector within the three wavebands 200-300μ, 300-400μ, 400-650μ. Principal sources considered are

Table 2

Source	temperature	emissivity

Telescope primary and secondary mirrors	**74 K**	**0.01**
4K optics direct to detector	**4 K**	**0.01**
2K optics direct to detector	**2 K**	**0.01**
2K enclosure walls direct to detector	**2 K**	**1.0**

The Blackbody intensities at each temperature T in each waveband are given below:

Table 3

	Blackbody intensity B(T,λ1,λ2), watt/cm^2/steradian, in waveband λ1->λ2		
T° K	**200-300m**	**300-400m**	**400-650m**
74	**1.17*10^-6**	**3.27*10^-7**	**2.0*10^-7**
4	**9.94*10^-13**	**8.21*10^-12**	**7.58*10^-11**
2	**2.78*10^-18**	**4.81*10^-16**	**1.25*10^-13**

The contributions from the primary and secondary mirrors are taken from APART analysis of the earlier SPIRE photometer model covered in the ESA report SPIRE/RAL/N/0101.01. Also taken from this report are the estimates (~6.0% of the total) for the contributions due to surfaces in the payload module that lie outside the SPIRE instrument. No allowance has been made for transmission losses in SPIRE optics.

The contributions from the optics in the 4K and 2K boxes are computed using

$$E(T, l1, l2) = N_M * A * \Omega * e_{optic} * B(T, l1, l2)$$

with N_M = the number of optical surfaces.

The contribution from the 2K surround is somewhat over-estimated using

$$E(T, l1, l2)_{suround} = p * A_{detector} * e_{surround} * B(T, l1, l2)$$

Table 4 summarises the results of the computations.

Table 4

	Signal in watts in-band		
Source	**200-300m**	**300-400m**	**400-650m**
Telescope optics	**2.4*19^-9**	**3.94*10^-9**	**14.04*10^-9**
6% of Telescope signal	**1.44*10^-10**	**2.36*10^-10**	**8.42*10^-10**
2K surround	**5.45*10^-17**	**9.43*10^-15**	**2.45*10^-12**
2K optics	**5.54*10^-21**	**9.61*10^-19**	**2.50*10^-16**
4K optics	**5.96*10^-15**	**4.93*10^-14**	**4.55*10^-13**

Compared to the contributions expected from the optics, the 2K surround direct contribution only becomes significant for the longer waveband. Even then, it is still significantly smaller than the total of the contributions expected from surfaces outside the instrument reaching the detector along the natural optical path through the SPIRE photometer.

4. GEOMETRICAL OPTICAL BEAM FOOTPRINTS

Geometrical optical beam footprints are now being redetermined, using the latest optical designs for the two instruments. Some of these are presented in the following figures. For each instrument, the centre and 24 points evenly spaced around the perimeter of a detector were used as field points. A rectangular detector (sized to be nominally 8 x 4 arc minutes on the sky) is used for the photometer and a circular detector (sized to be nominally 1.3 arc minutes radius on the sky) is used for the spectrometer. Each instrument’s footprint is therefore made up of 25 separate beams. The rays determining the footprints were traced from each detector outwards, passing through each instrument’s aperture stop, to space, so that the footprints represent regions of surfaces viewable from different points on the edge of a detector.

The view that each detector has of surfaces from CM4 outwards to the telescope is complicated by the necessity to use CM4 to ‘chop’ the photometer view by up to +-2 arc minutes on the sky at 90 degrees to the fold plane and by up to +-30 arc seconds on the sky in the fold plane. Since the spectrometer optical path uses the same optical surfaces as the photometer from CM5 outwards, its detector’s view will also be chopped.

4.1 Composite beams between SPIRE mirror CM3 and the telescope's secondary mirror M2

A. This shows the minimum size required for CM3 to cover the geometrical beams for the full range of tilts currently envisaged for the steering mirror CM4.

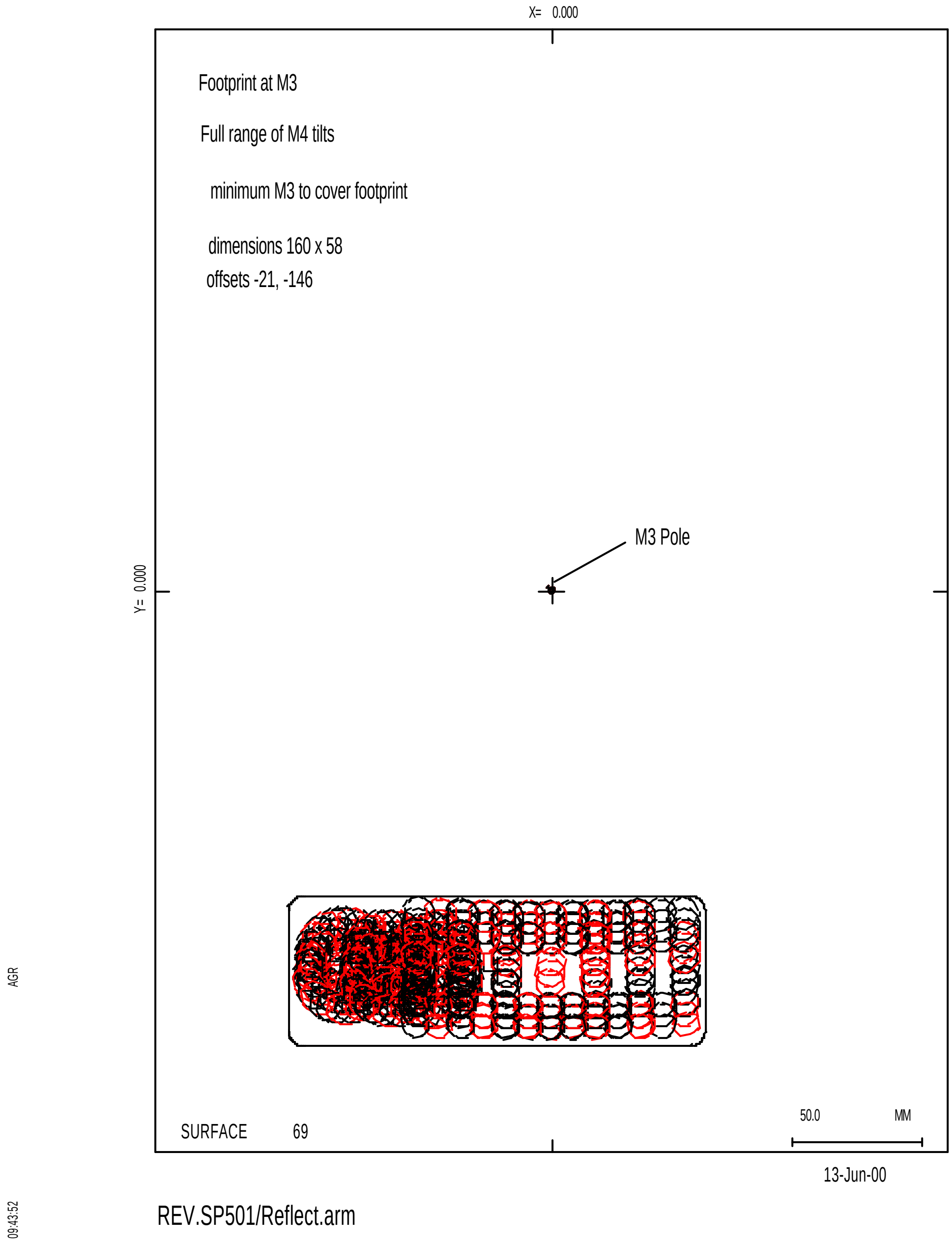

B. This shows the minimum size required for an aperture located in a plane 27 mm forwards of the telescope axial focus (26.6 mm is the sag of the 167.171 mm radius curved telescope focal surface at the SPIRE off-axis distance of 90.5 mm). This aperture just transmits the two fields of view. It will begin to vignette and occlude beams from some areas of each detector as CM4 is tilted over its full range.

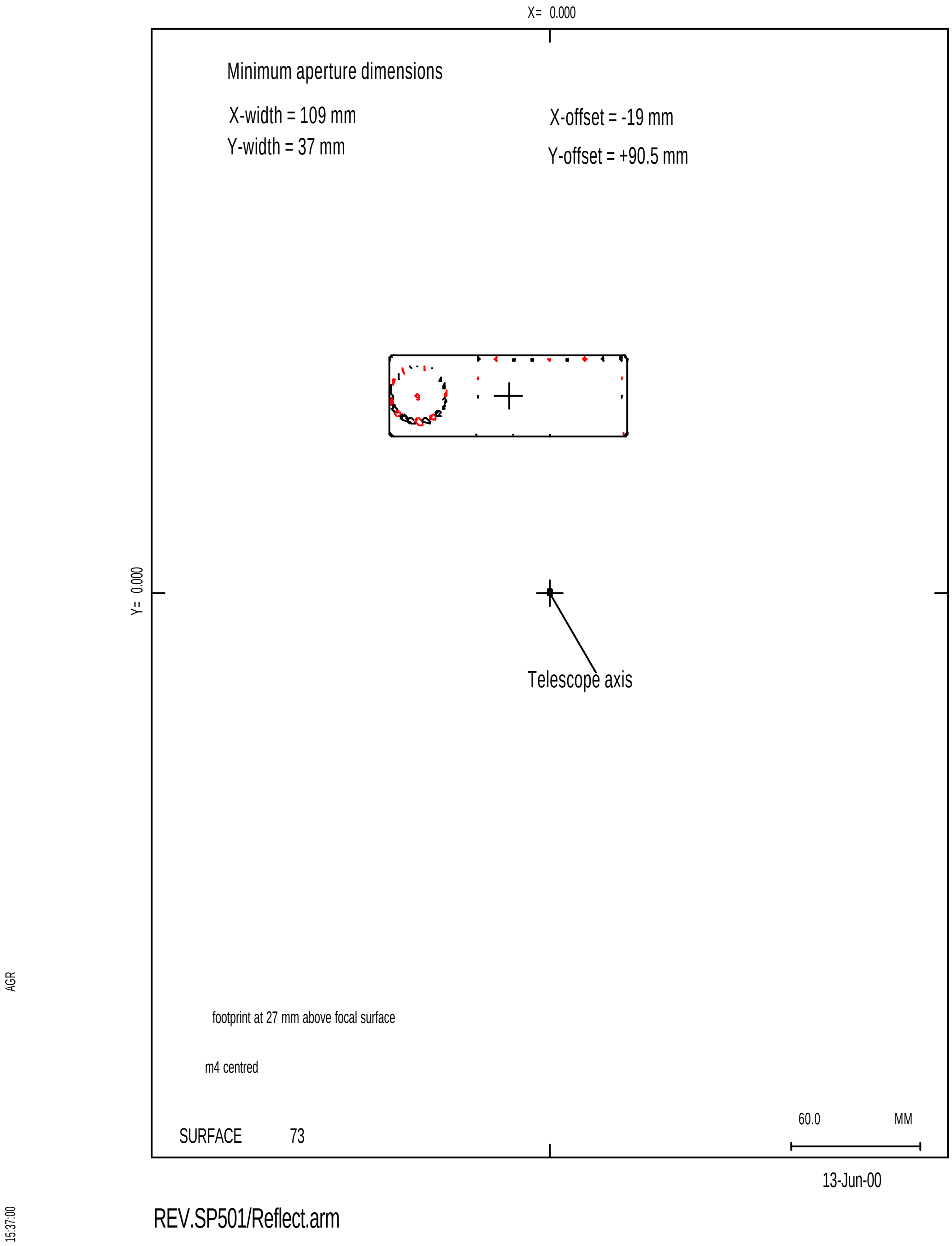

C. This shows the effect the aperture will have when CM4 tilts the instrument fields of view over their full range. If CM3 is suitably oversized, then some parts of the detectors will view the rear of this aperture as CM4 is tilted.

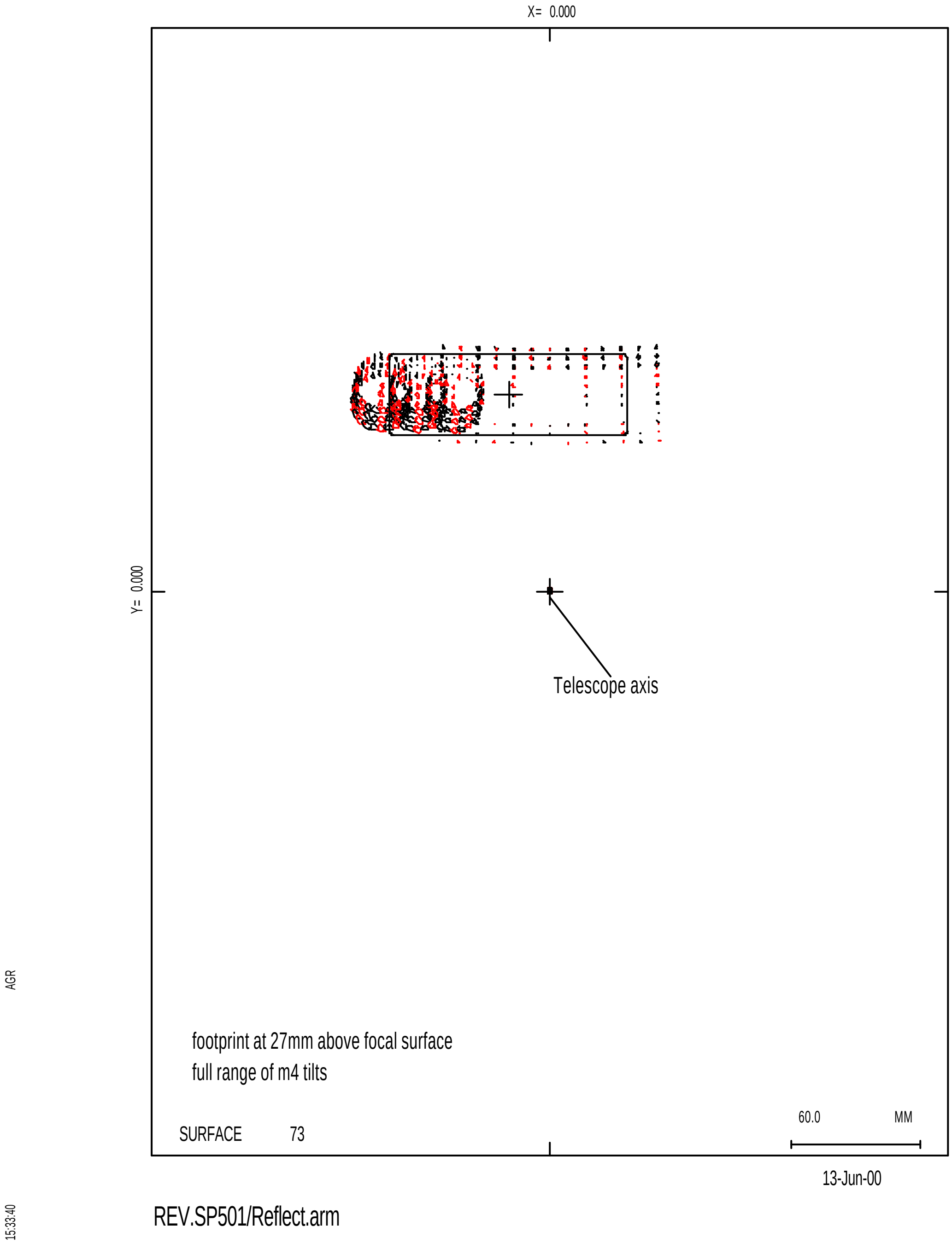

D. This shows how spectrometer detectors may begin to 'see' cryostat edges/surfaces, as CM4 is tilted over its full range, if there is no field stop at the focal surface. N.B. The original cryostat model had a 130 mm radius 'bore', resulting in almost certain encroachment into the spectrometer's detectors' field of view with the present designs for SPIRE and telescope.

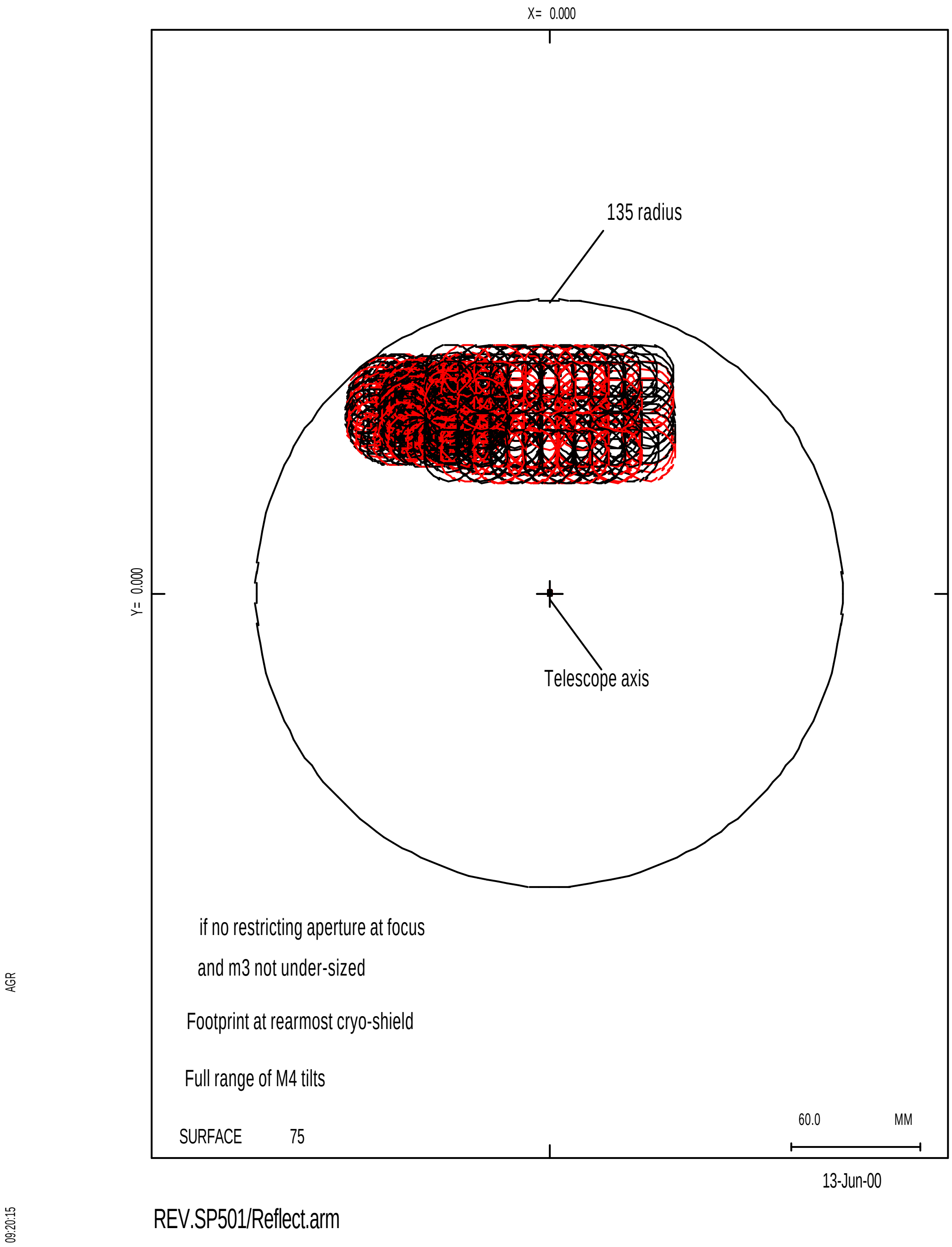

E. This shows how spectrometer detectors may begin to 'see' primary mirror hole edges/surfaces, as CM4 is tilted over its full range, if there is no field stop at the focal surface. N.B. the latest telescope design demands a minimum hole radius = 134.5 mm (required to pass 0.25 degree unvignetted FOV) and a maximum radius = 146 mm (prevent rays within FOV passing directly to focal surface without hitting the primary).

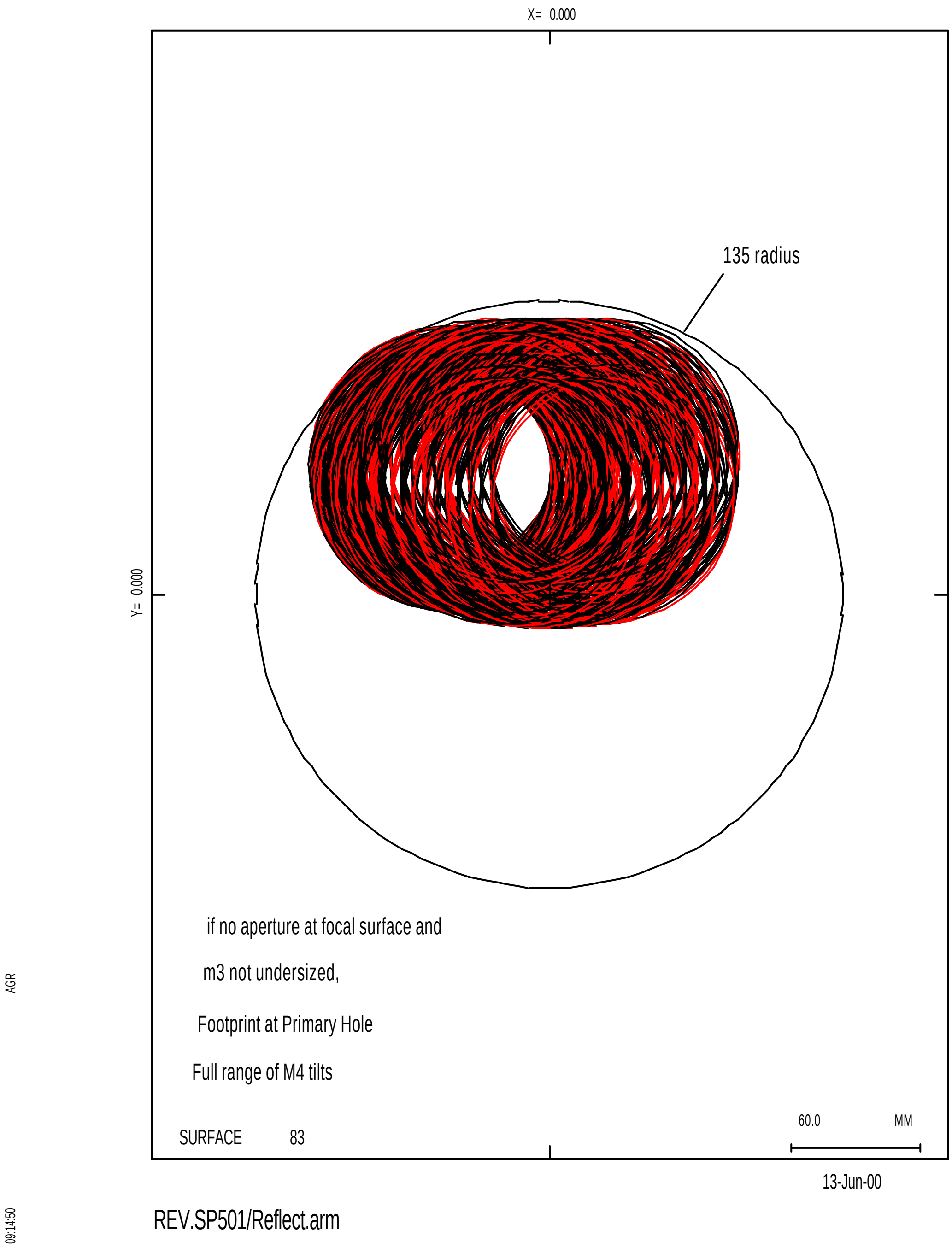

F. This shows how a spectrometer detector's view can wander over the edge of the telescope secondary mirror,M2, if there is no field stop at the telescope focal surface. M2's design radius is 154.15 mm. The photometer geometrical footprint remains just inside the boundary of M2.

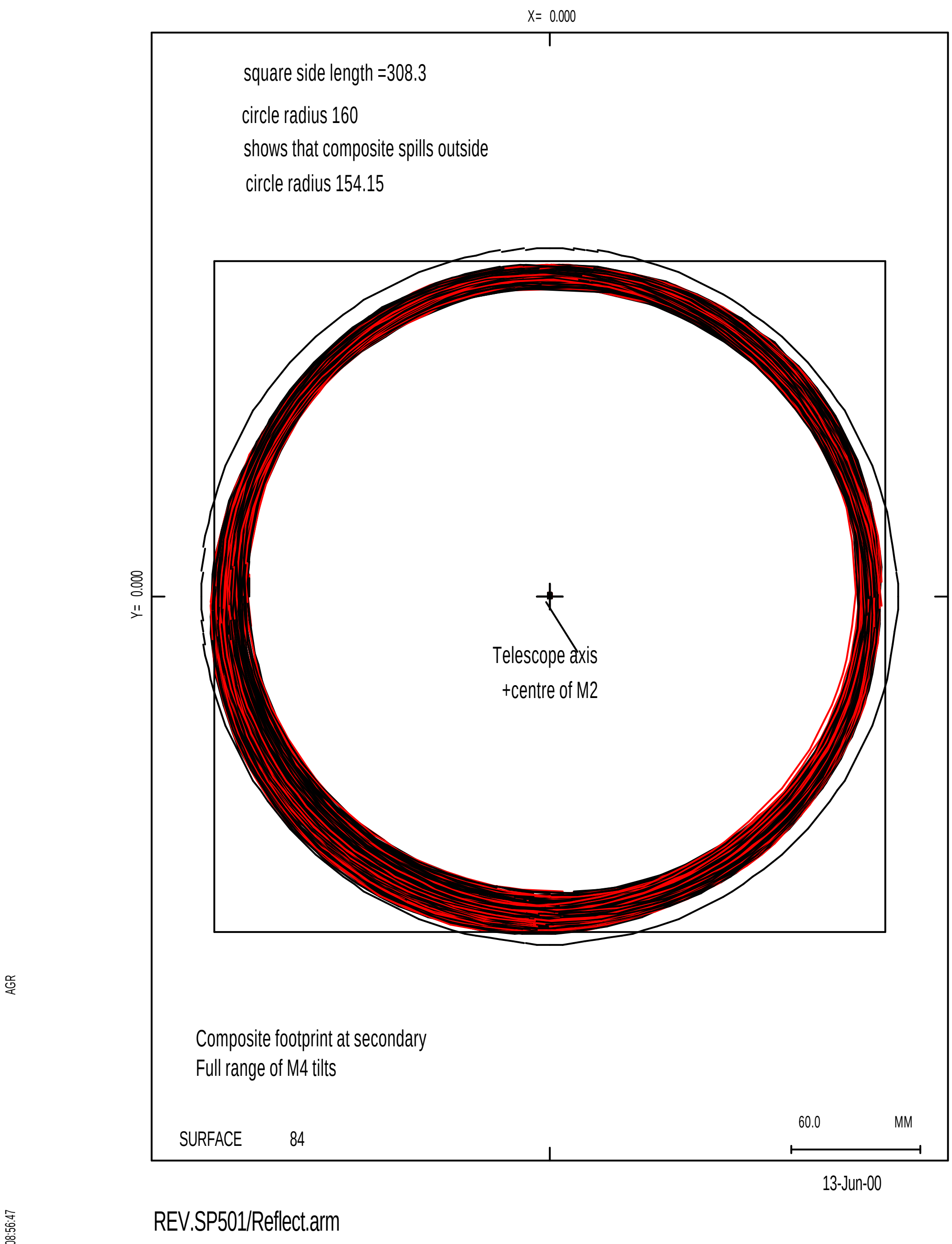

4.2 Composite Geometrical Optical Beams in the common path between M5 and M3

A. Minimum size required for CM3 if it is to cover the fully chopped/jiggled field of view of both instruments.

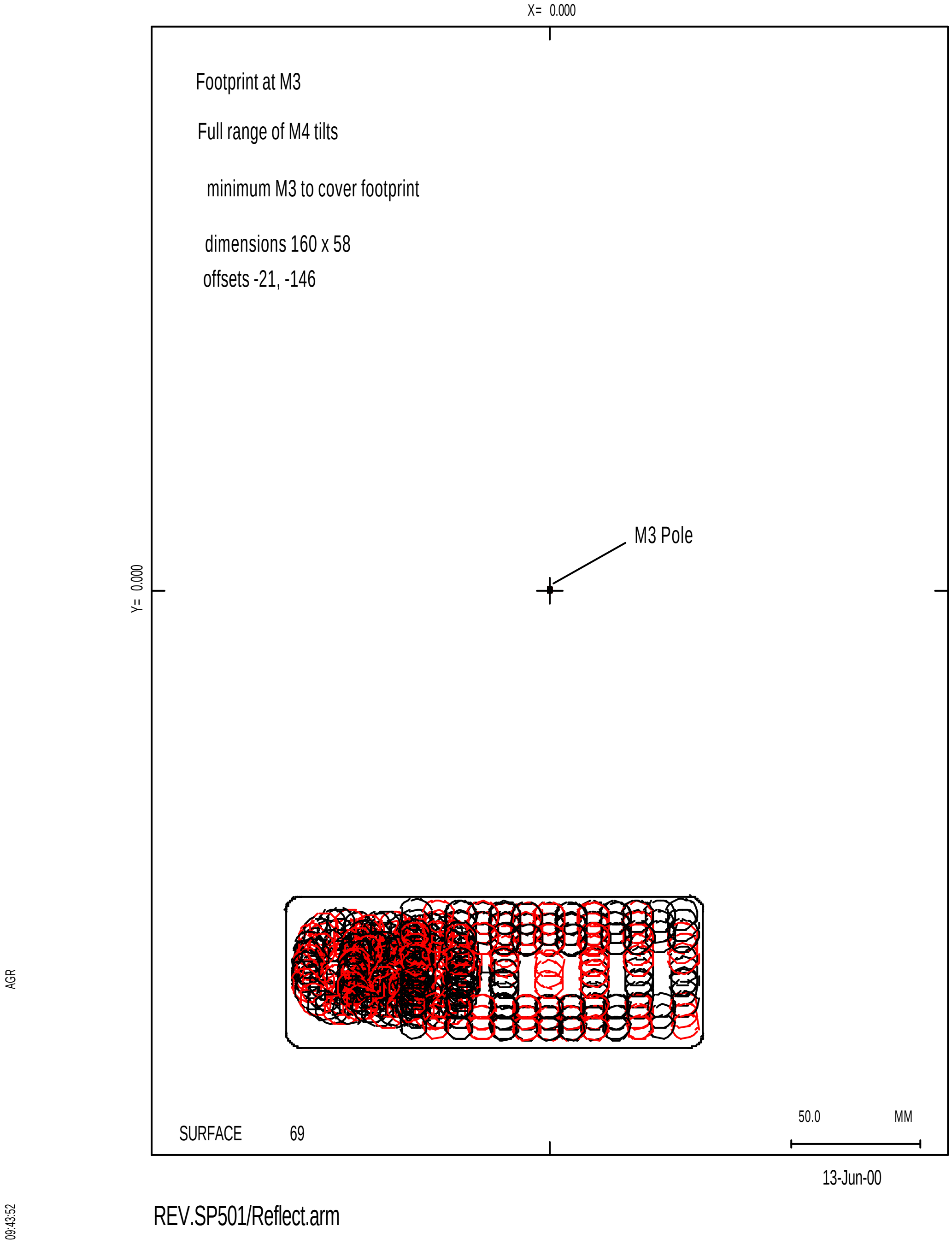

B. Minimum size required for CM4 if it is to cover the fully chopped/jiggled field of view of both instruments. The asymmetry is caused by the poorer spectrometer pupil imagery.

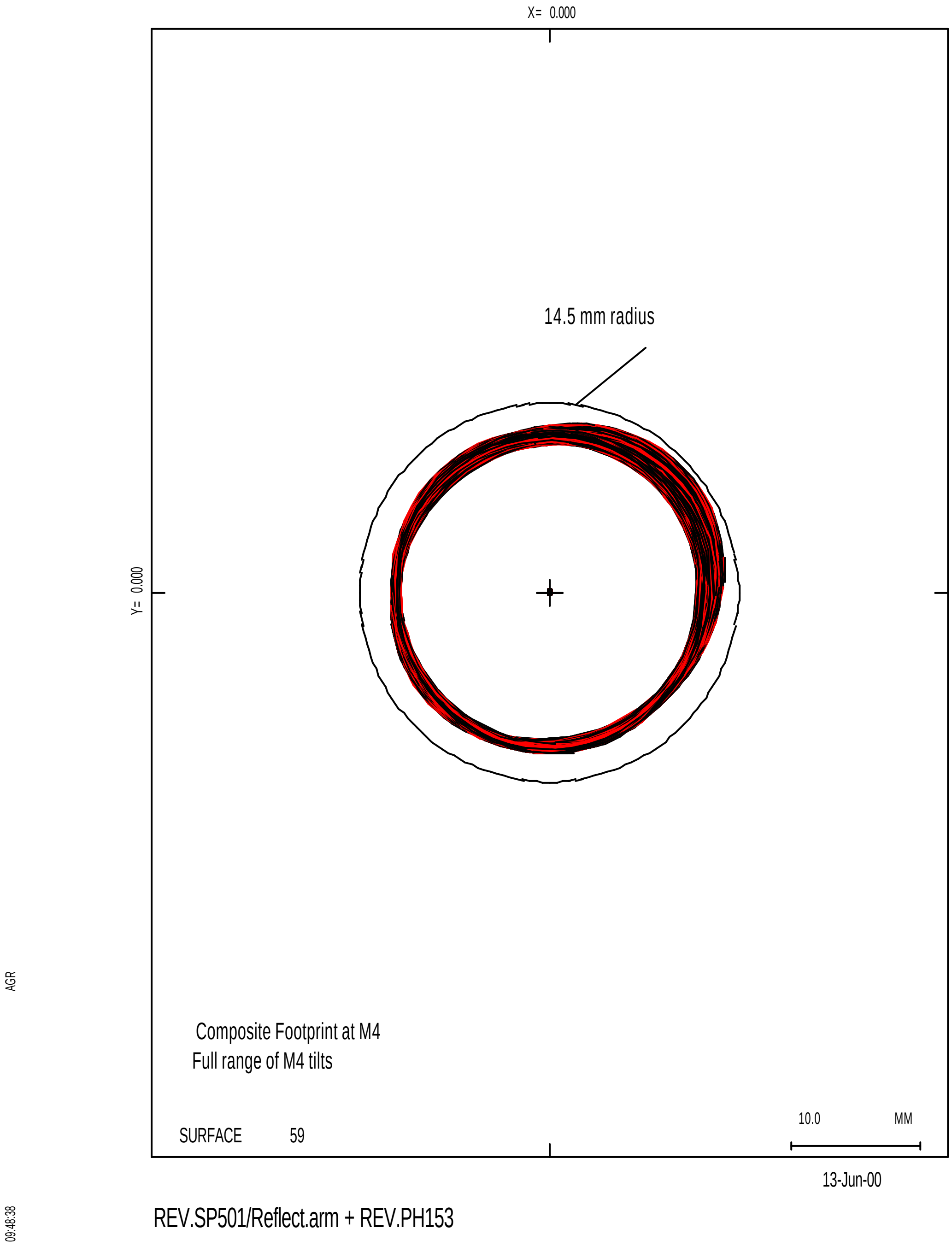

C. Minimum size required for CM5 if it is to cover the fully chopped/jiggled field of view of both instruments.

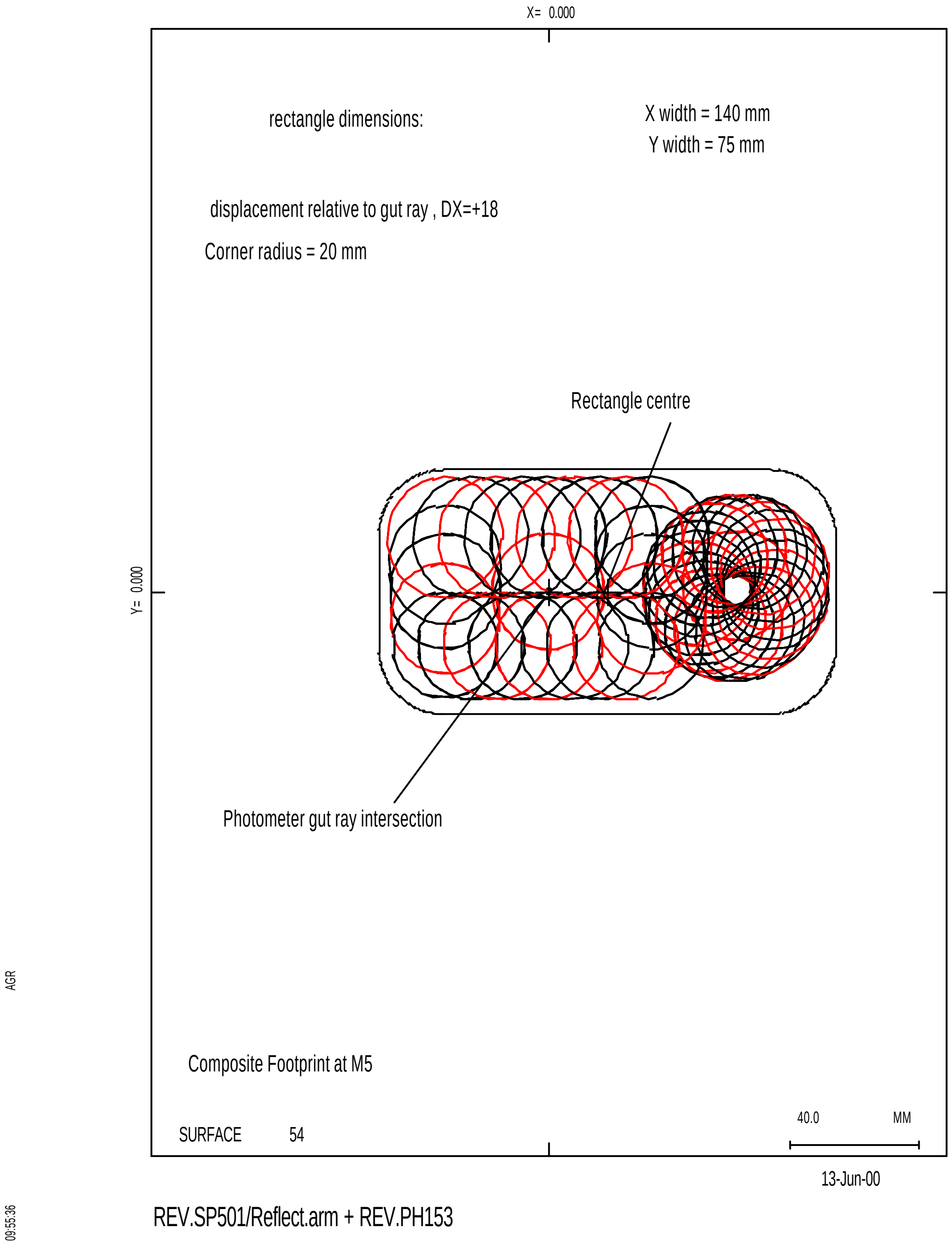

4.3 Geometrical optical beam footprints of a detector field of view at Photometer mirrors

A. Field mirror PM6

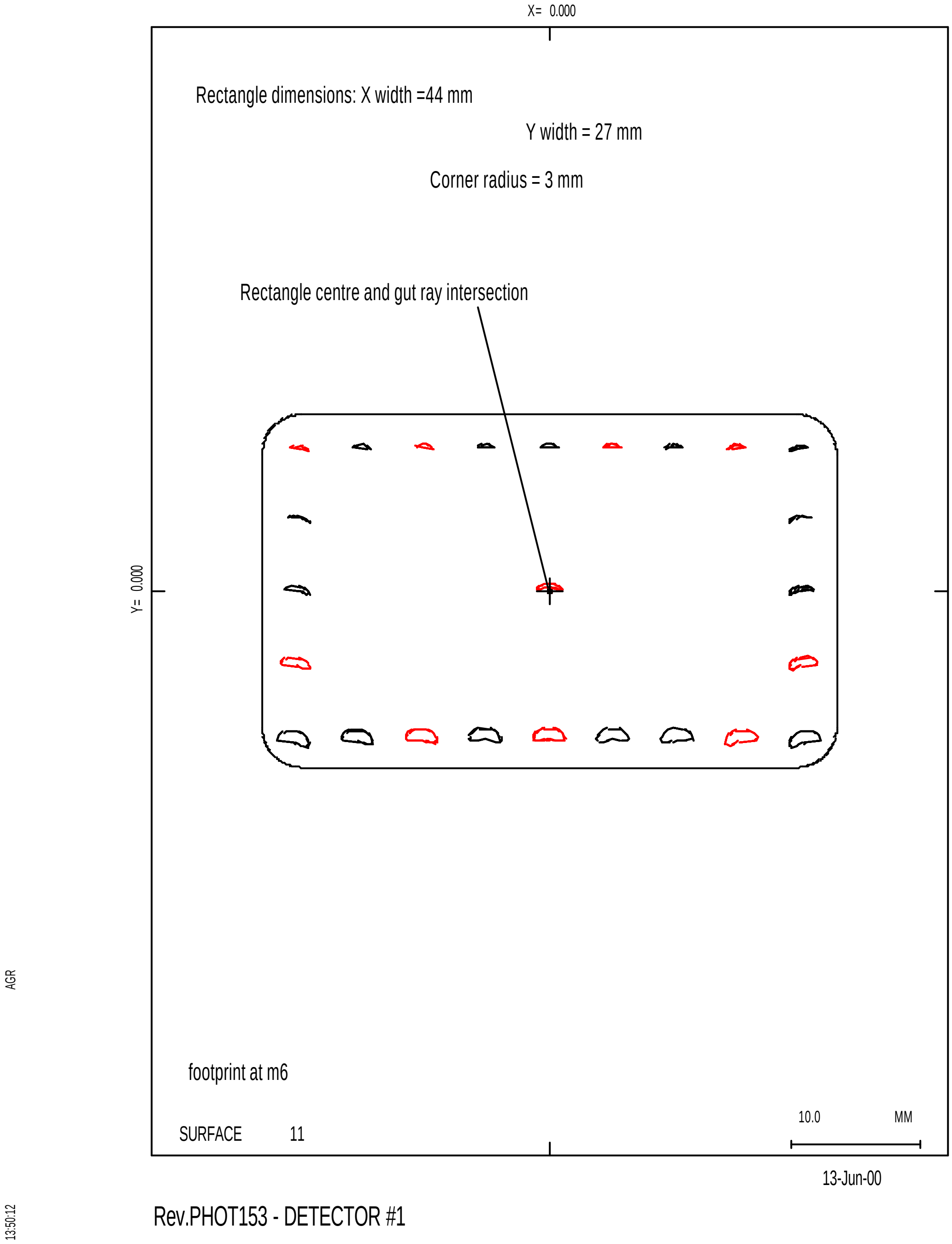

B. Mirror PM7

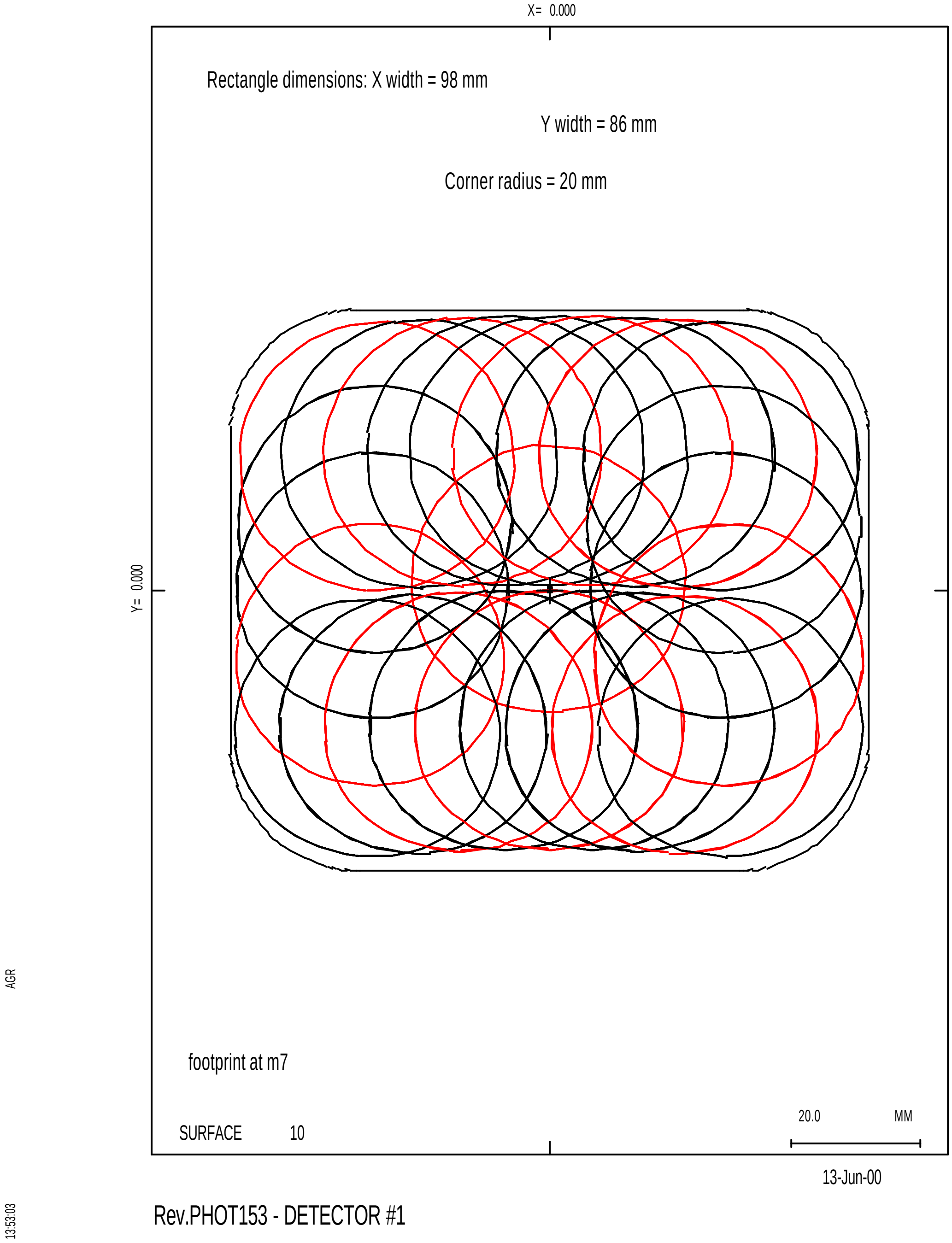
X= 0.000
Rectangle dimensions: X width = 98 mm
Y width = 86 mm
Corner radius = 20 mm
Y= 0.000
AGR
footprint at m7
SURFACE 10
20.0 MM
13-Jun-00
13:53:03
Rev.PHOT153 - DETECTOR #1

C. Mirror PM8

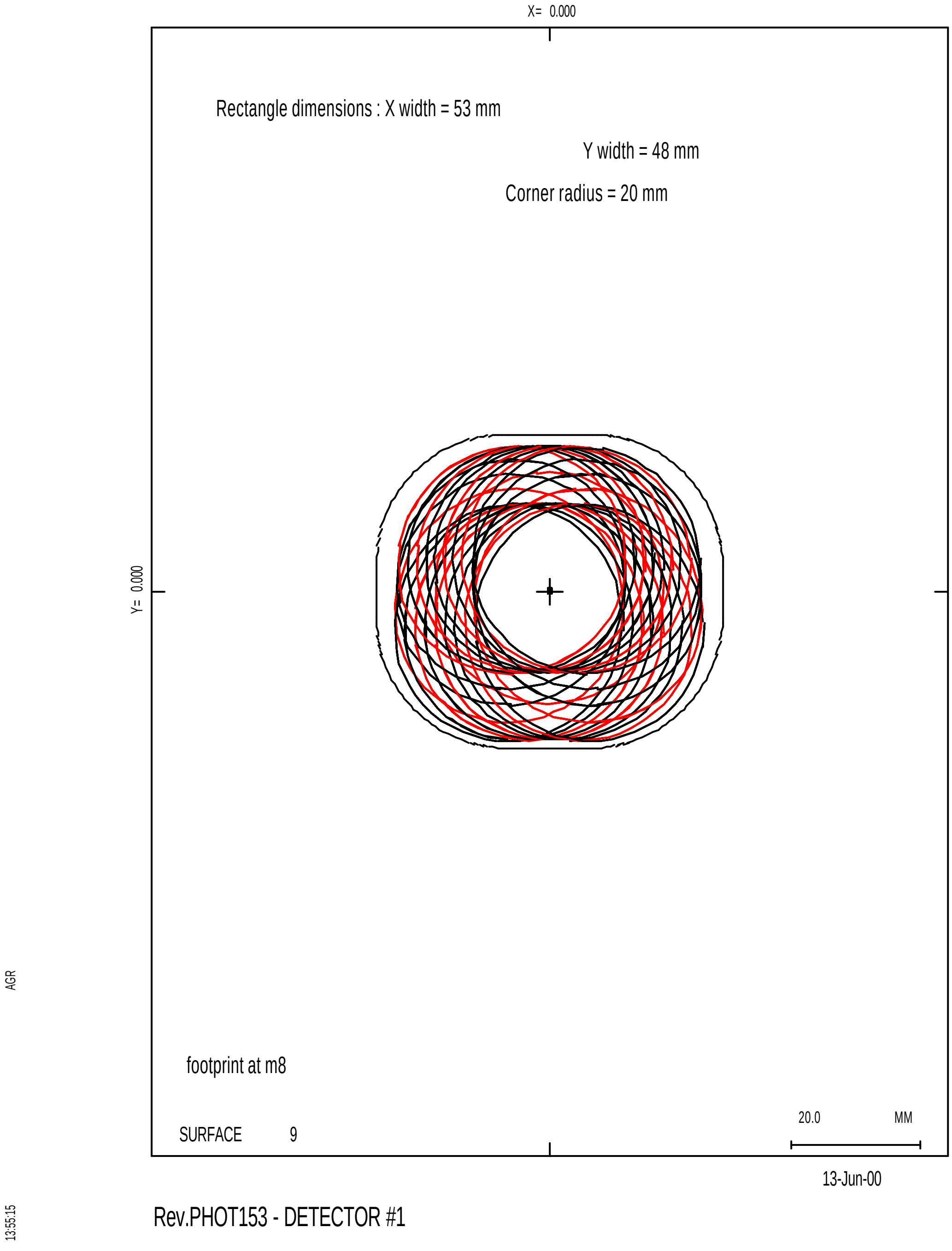
X= 0.000
Rectangle dimensions : X width = 53 mm
Y width = 48 mm
Corner radius = 20 mm
Y= 0.000
AGR
footprint at m8
SURFACE 9
20.0 MM
13-Jun-00
13:55:15
Rev.PHOT153 - DETECTOR #1

D. Mirror PM9

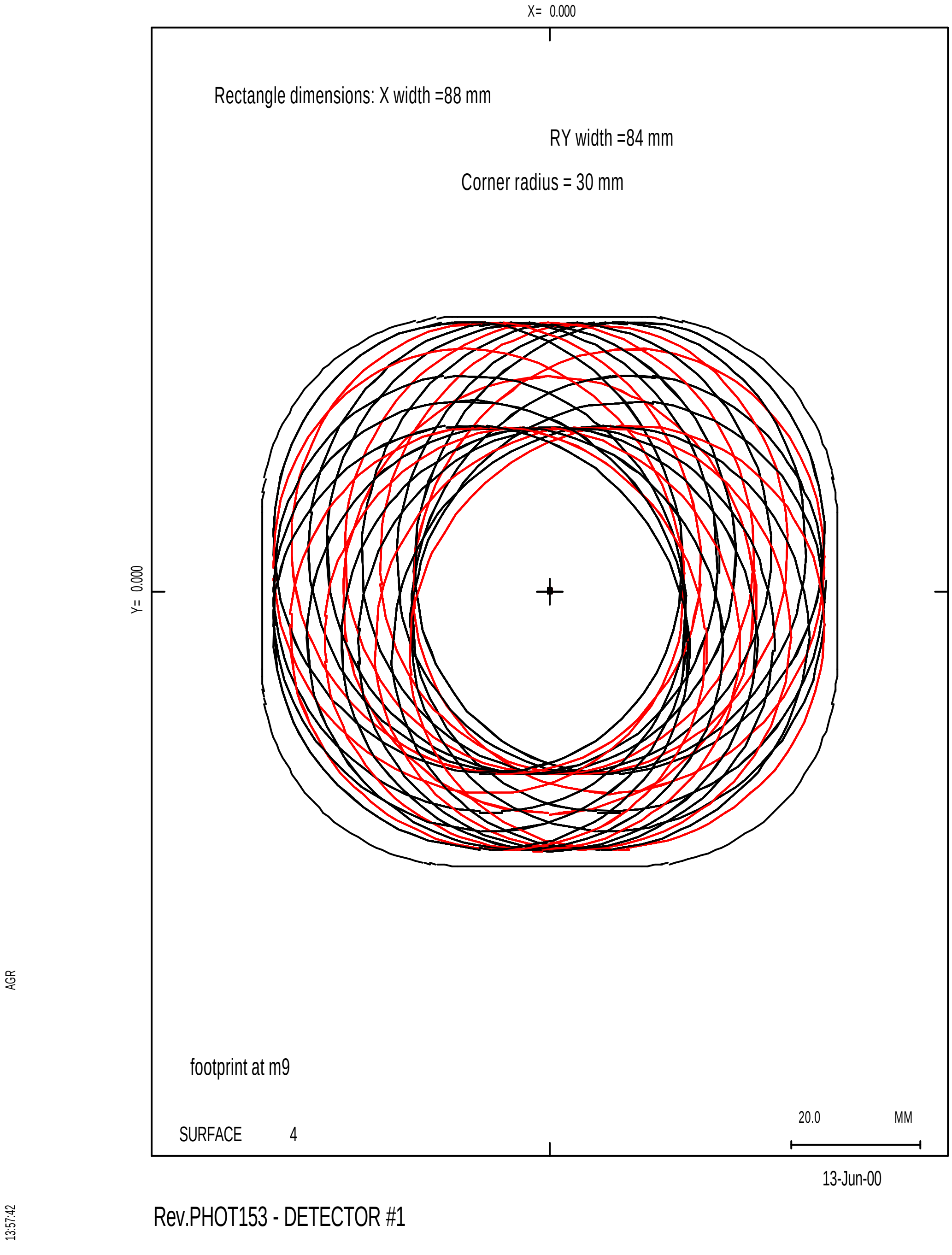
X= 0.000
Rectangle dimensions: X width =88 mm
RY width =84 mm
Corner radius = 30 mm
Y= 0.000
AGR
footprint at m9
SURFACE 4
20.0 MM
13-Jun-00
13:57:42
Rev.PHOT153 - DETECTOR #1

4.4 Geometrical optical beam footprints in one arm of the Spectrometer

These figures show the effects, at locations in one arm of the spectrometer (the arm that views space by reflection from SBS1), of moving the Corner cube from +3 to –32 mm from its zero-path difference position

A. Fold mirror SM12A.

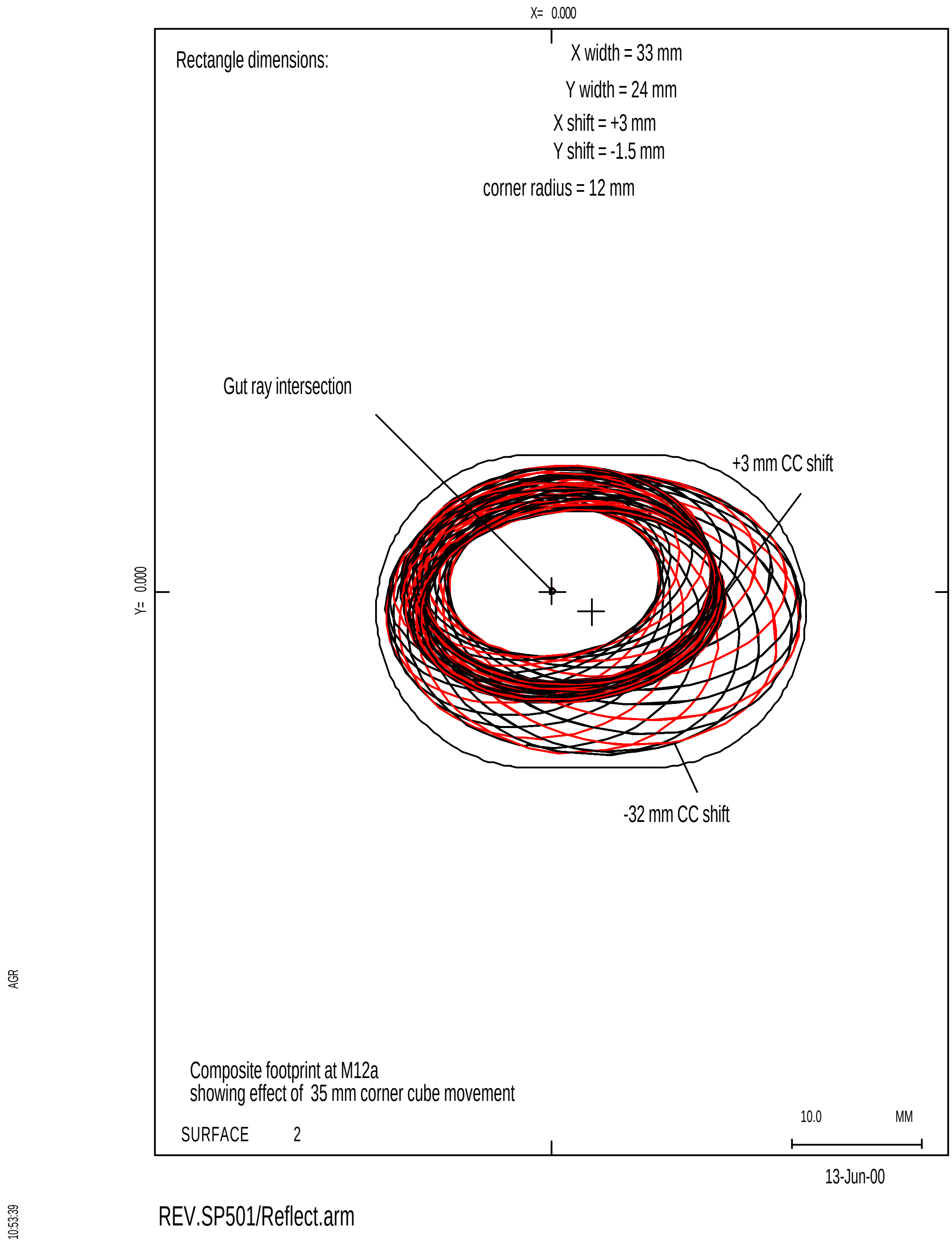

B. Camera mirror SM11A.

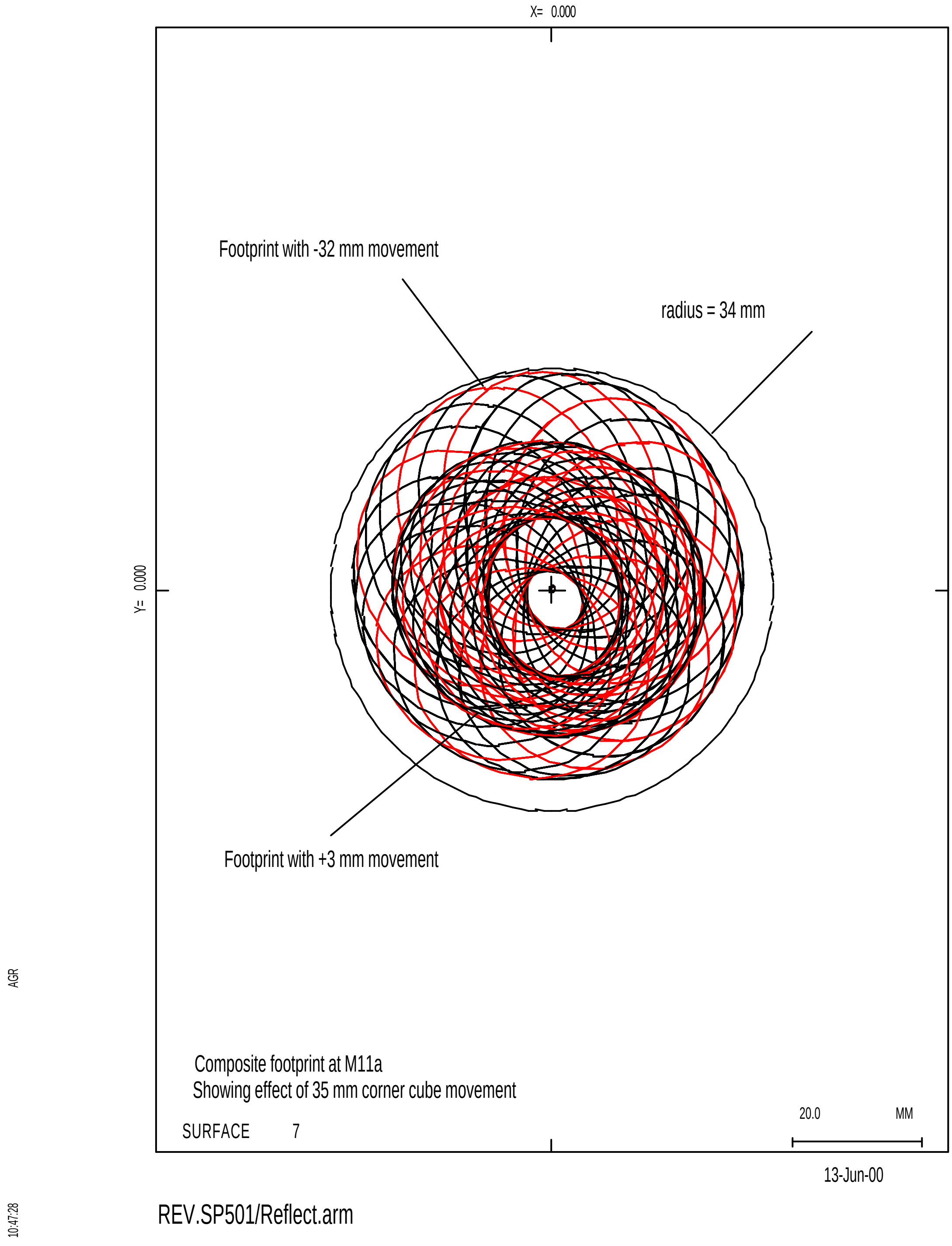

C. Beam splitter SBS2.

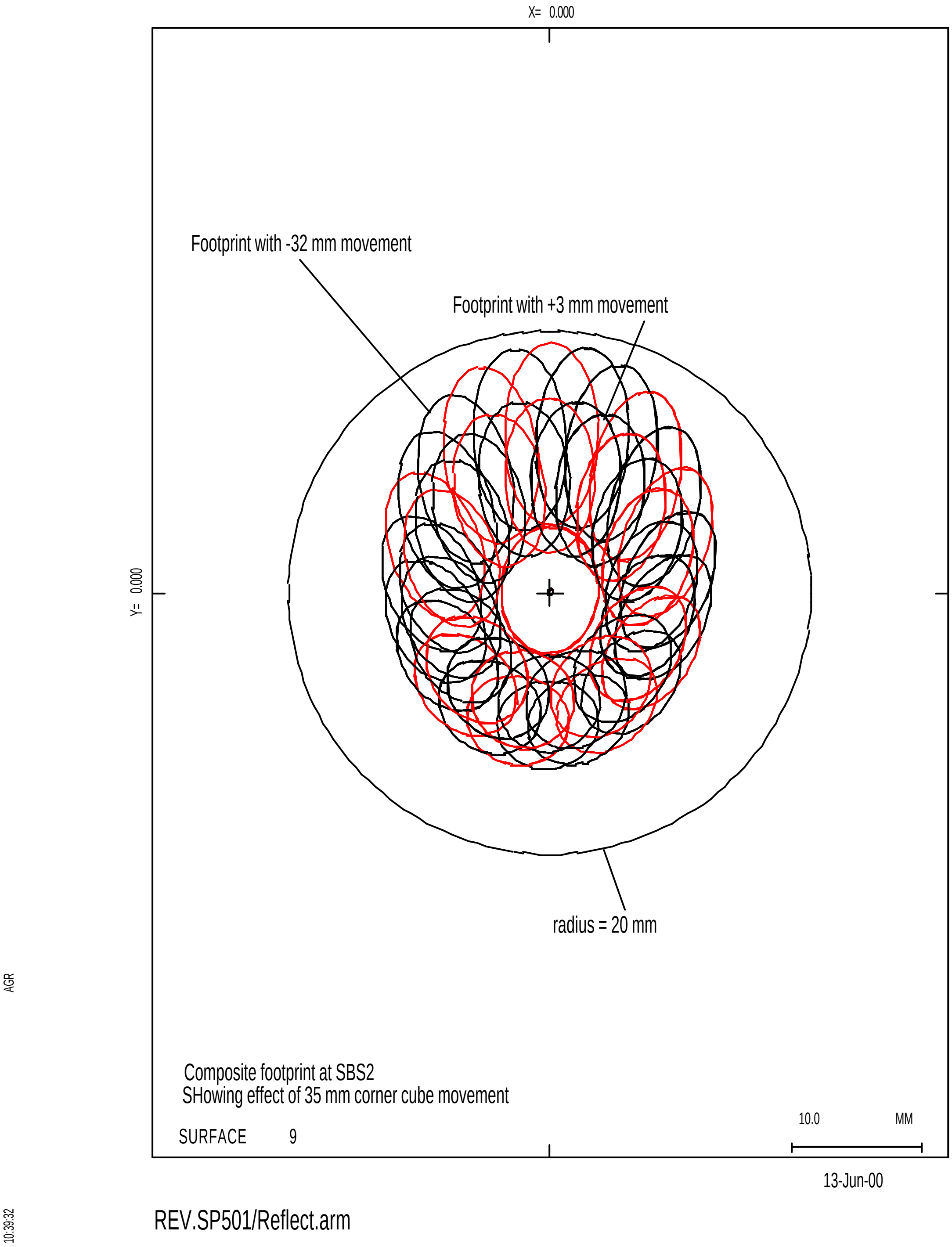

D. Collimator mirror SM10A.

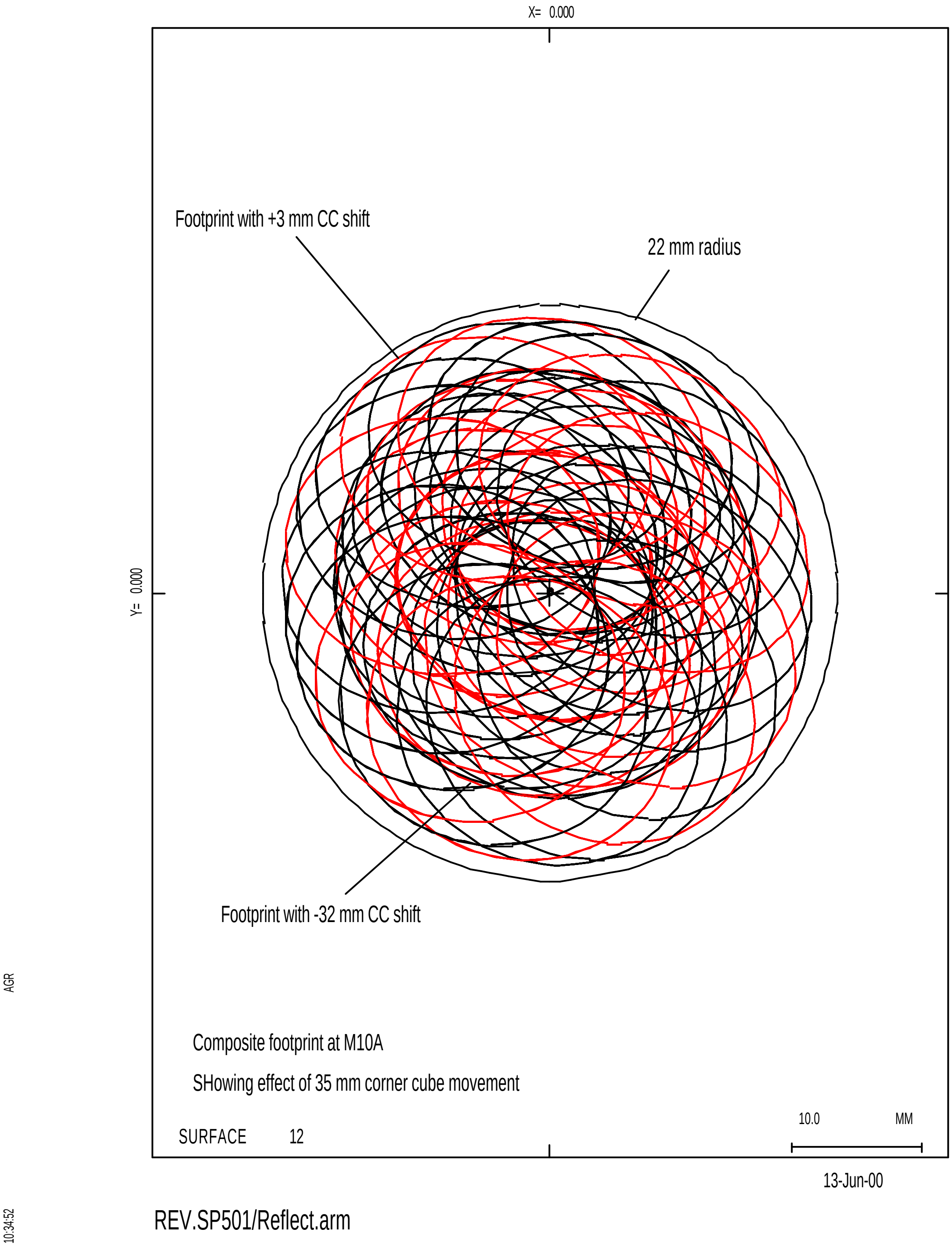

E. Collimator mirror SM9A.

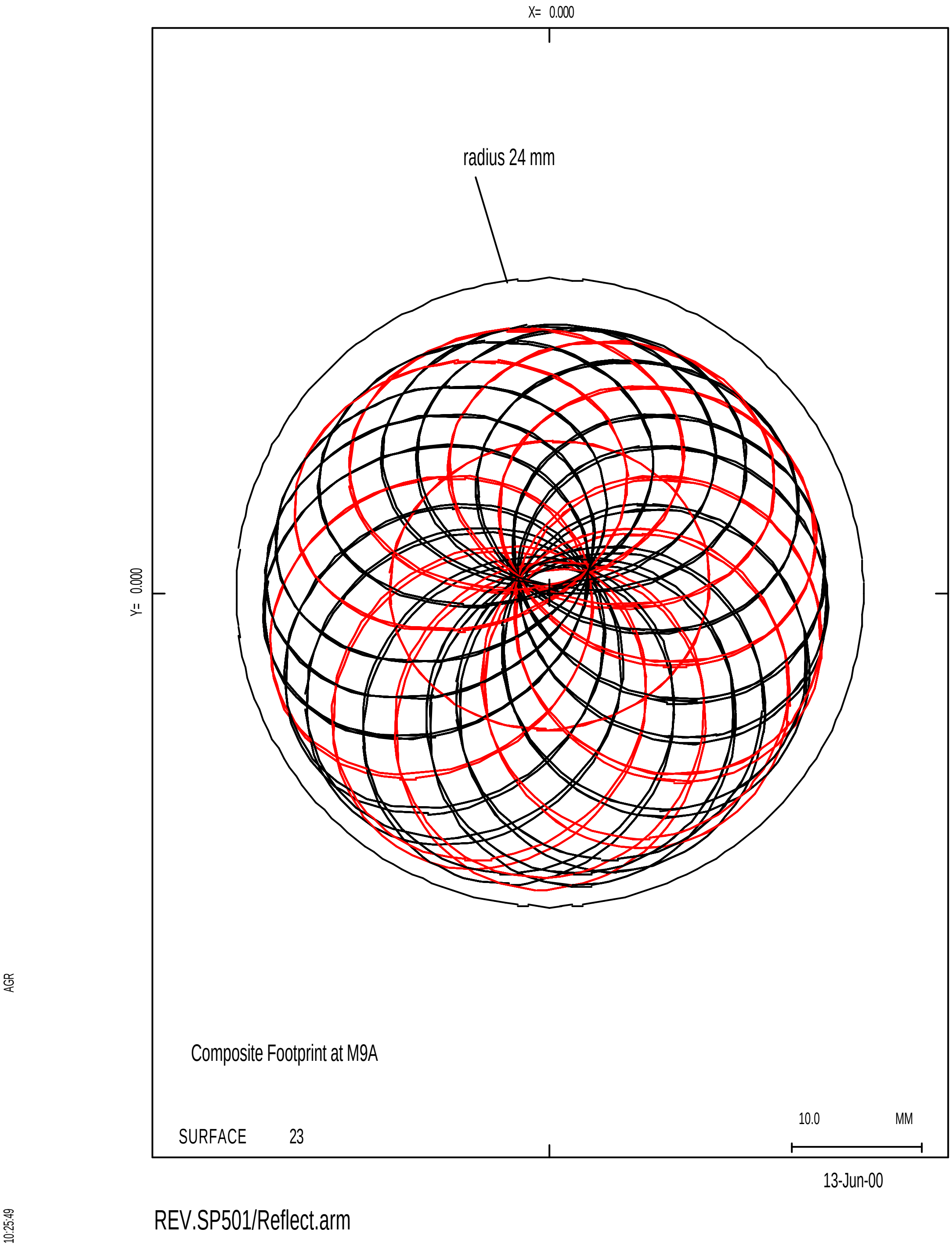

F. Beamsplitter SBS1A.

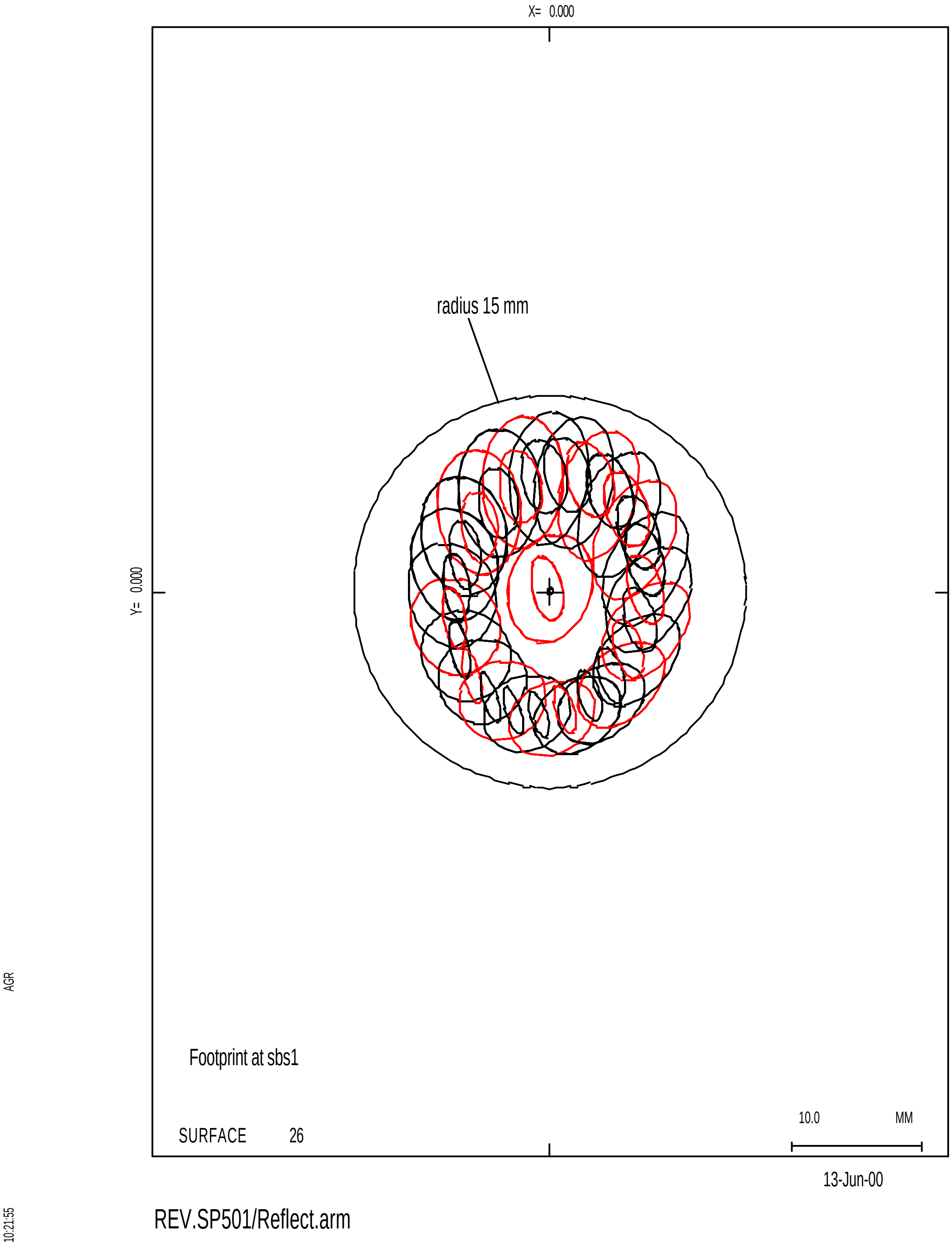

G. Camera mirror SM8A.

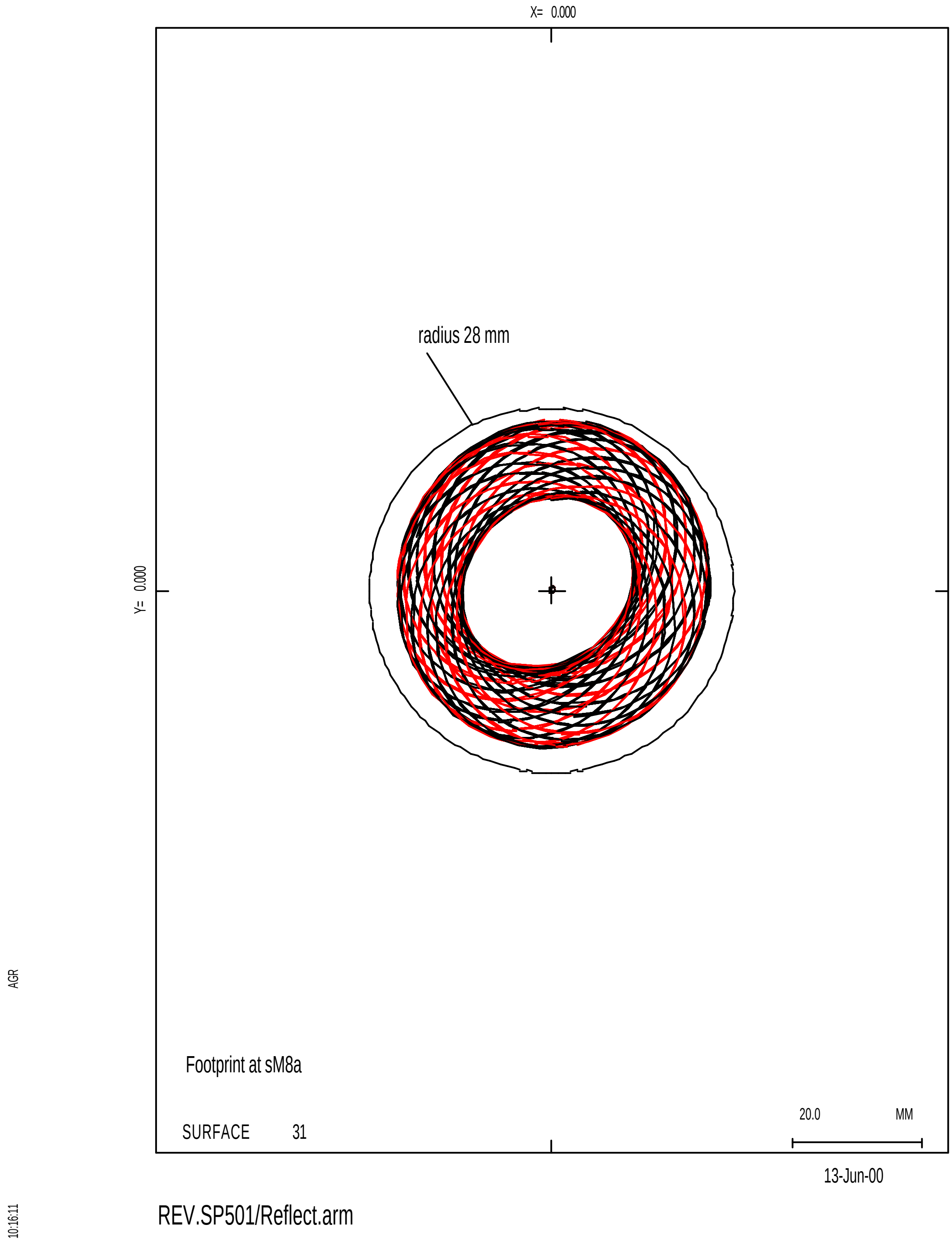

H. Flat mirror SM7A.

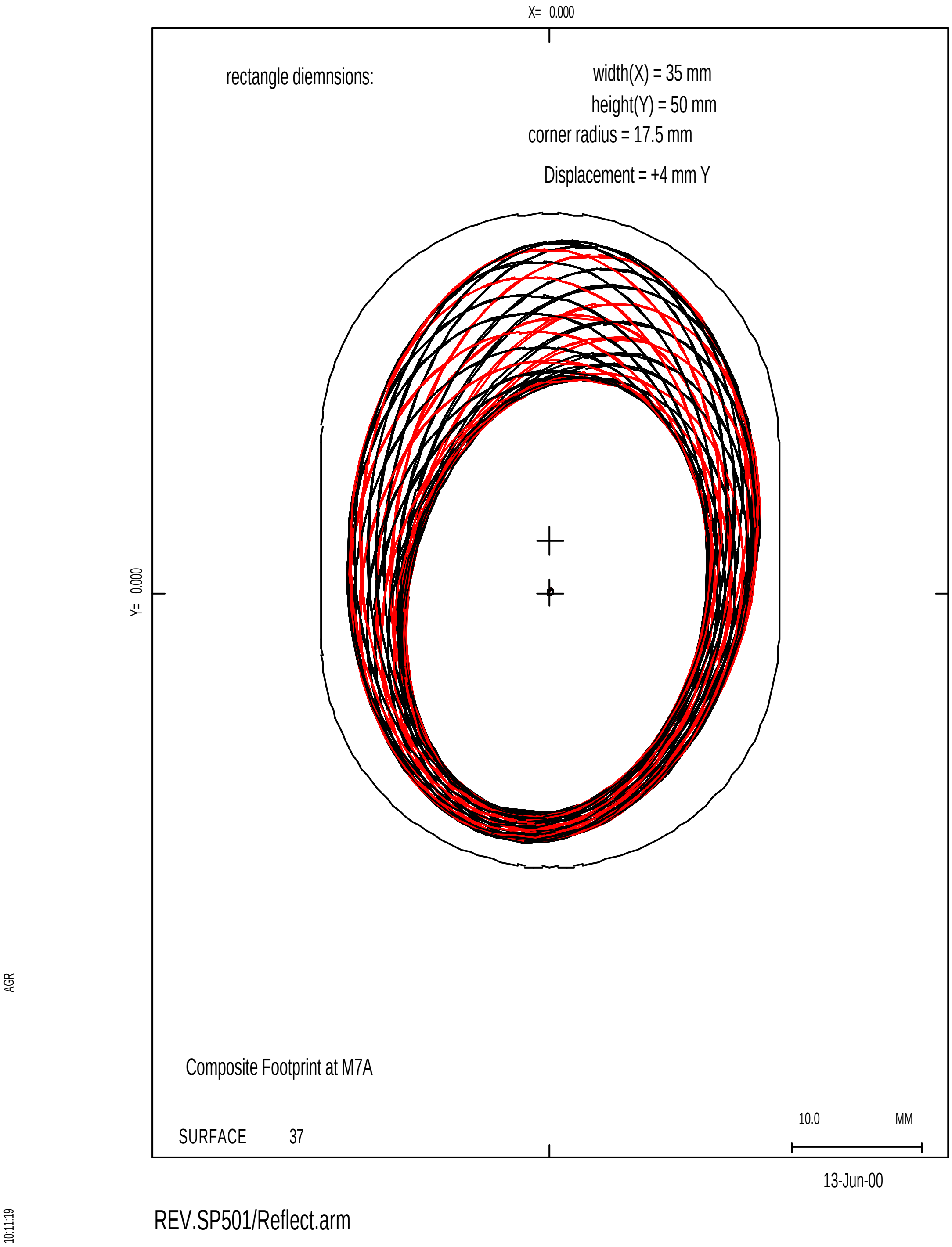

I. Field mirror SM6A.